

Flow structure of the plane turbulent impinging jet in cross flow

Structure de l'écoulement de l'impact d'un jet plan turbulent dans un courant traversier

MEILAN QI, *PHD Student, Dept. of Hydr. Eng., Tsinghua Univ., China.*

ZHICONG CHEN, *Prof., Dept. of Hydr. Eng., Tsinghua Univ., Beijing 100084, China.*

RENSHOU FU, *Prof., Dept. of Hydr. Eng., Tsinghua Univ., Beijing 100084, China.*

KEY WORDS: Normal impinging jet, cross flow, turbulence, velocity similarity

MOTS-CLES : Jet incident normal, écoulement transverse, turbulence, similitude de vitesse.

ABSTRACT

This paper presents both experiment and numerical simulation on Two-dimensional vertical impinging jet in cross flow. Intake pond of the cooling water system is a requisite component of thermal or nuclear power plant. But in intake pond sediment deposition is heavy. Impinging jet was equipped in a nuclear power plant in China and has a significant impact on sediment suspension. However, before this investigation, little attention has been paid to the mechanism of this application case. In response to the demands of the engineering design, started this study. Experiments are performed for different Reynolds number ratio of the jet-to-cross-flow R varying from 0.13 to 0.22. The measurement results of turbulent parameter and flow structure are obtained. Moreover the turbulent parameters play an important role on sediment transportation. As well the experiment results agree well with the calculations provided from $\kappa - \epsilon$ turbulence model.

RÉSUMÉ

Cet article présente une simulation à la fois expérimentale et numérique d'un jet vertical bidimensionnel impactant dans un courant transverse. Le bassin d'alimentation des systèmes de refroidissement est un composant indispensable des centrales thermiques ou nucléaires, mais, dans ces bassins, les dépôts de sédiments sont pénalisants. En Chine, une centrale nucléaire a été équipée d'un jet impactant qui a joué un rôle significatif sur la mise en suspension de sédiments. Peu d'attention avait été prêtée auparavant au mécanisme de ce cas d'application. Cette étude a donc été entreprise pour répondre aux besoins de la conception technologique. Les expériences sont menées pour différents rapports de nombres de Reynolds, entre le jet et le courant transverse, variant entre 0.13 et 0.22, et ont fourni des mesures des paramètres turbulents et de la structure de l'écoulement. De plus, les paramètres turbulents jouent un rôle important sur le transport de sédiments. Les résultats expérimentaux sont en bon accord avec les résultats numériques obtenus dans un modèle de turbulence $\kappa - \epsilon$.

Introduction

As a favorable measure, jet is widely employed in solving siltation problem in hydraulic engineering. For example, intake pond of cooling water system is a requisite component of thermal or nuclear power plant. And in the whole intake pond where the flow section is expanded compared to the connection between the intake pond and outer, sediment frequently deposits due to the reduction of the flow velocity. With sediment laden flow continuously coming and sediment depositing, the siltation at the bottom is thickened and, consequently, the pump doesn't work. In consideration of this situation, a significant and new measure, vertical impinging jet, was employed in a power plant in China to prevent the sediment from depositing and an effective result was achieved (Chen, 1997). However, little attention has been paid to the mechanism of this practical case. Moreover the mechanism is essential to the increasingly application of this measure to the engineering. For this reason, this paper presents the flow structure by the results of experiments and numerical computations.

Research on erosion by jets has been mainly empirical because of the complex nature of the flow and its intersection with the mobile bed. Beltaos (1973), (1977) studied turbulent jet impinging on a solid surface. Rajaratnam (1977), Kobus (1979), studied turbulent jet impinging on a sand bed. These studies of the impinging jet were mainly by experiments, including empirical in-

formation. Turbulent horizontal jets in stagnant and coflowing surroundings were studied theoretically and experimentally (Abramovich (1963) and Rajaratnam (1976)). McGuirk and Rodi (1978) calculated the near field of the side discharge over the full depth into a straight channel using depth-averaged two-dimensional model. But so far, there are few studies for the turbulent jet issuing vertically downward into cross open channel flow and impinging on solid bed. For this reason, this paper presents some experimental results of the flow structure and turbulence information with a comparison of numerical calculations of the mean and fluctuating velocity components. This investigation has also been used in practical engineering problem in intake pond of cooling water system of a power station.

Experimental and Numerical Method

Experimental Setup

The experiments are performed in a glass flume in the sediment laboratory of the department of hydraulic engineering of Tsinghua University. The experimental setup is shown in Fig.1. The dimensions of the flume test section are 700-cm long, 25-cm wide and 23-cm high. The Manning roughness coefficient (n) of bottom of the flume is 0.008. Jet nozzle is located at 400cm apart

Revision received November 8, 2000. Open for discussion till October 31, 2001.

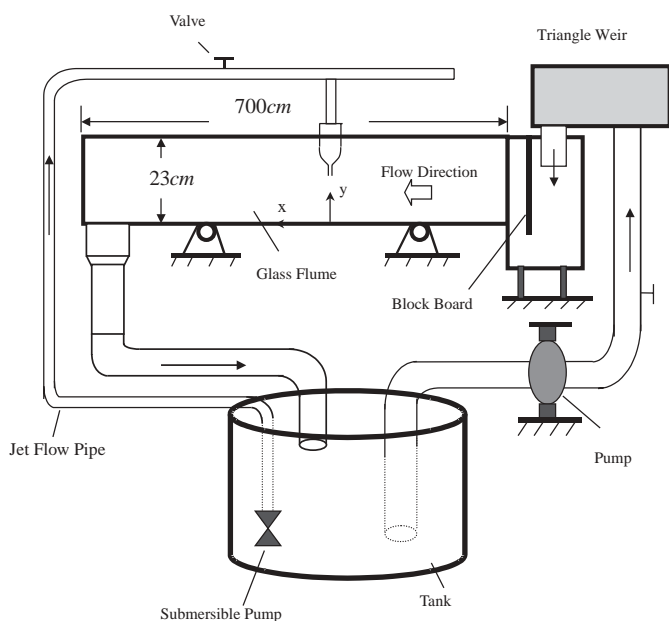


Fig. 1. Sketch of Experimental Setup

from the flume entrance. The x and y directions of the coordinates are respectively corresponding to the flume stream direction and the depth of the flume water. The origin of the coordinate is located at the bottom of the flume as shown in figure 1. The flume flow is supplied from a water tank by a pump and measured by a triangle weir. The flume with glass sidewall is slope adjustable. In this experiment, the slope of the flume is 0.001. The flow of the jet exit is supplied from a pressure box with a nozzle of 0.6mm in width (δ) and 25cm in length (B , which is equal to the flume width) which is installed across the flume in order to produce vertical plane impinging jet. In order to produce vertical two-dimensional jet flow, a very thin nozzle is adopted in this experiment. The nozzle is adjustable in height and is always kept just below the water surface to prevent air from entering the flume flow. The velocity of the jet at the nozzle, V_j , is measured by water head H_j .

Instrument

A point gage with a dial indicator is attached to the transverse rail of a carriage and could be moved to any point of the flume to measure the depth of the flow. An LDV instrument with wavelength of $0.6328 \mu\text{m}$ and measuring point diameter of $60 \mu\text{m}$ is used to achieve the two components of mean and fluctuating velocities. In the experimental processes, sufficiently long data records are obtained by LDV instrument in order to assume accurate time averages and the components of velocity intensity. All of the experimental results are repeatable within an error range of 5%.

Experiment Conditions

Data from 24 runs in a flume flow Reynolds numbers range 4000 to 20000 are included in this experiment. In the common sense, the flume flow Reynolds number is

$$Re = \frac{UH}{\nu} \quad (1)$$

where U being the mean velocity of the flume flow, H , the depth of the flow and ν , the kinematic viscosity of the fluid. For each of Reynolds number of the flume flow, jet velocities at the nozzle vary from 2.87m/s to 6.819m/s. In this paper, part of the experimental results for only one case of flume Reynolds number are presented. The depth of the flow is maintained at 10cm. Other significant parameters of the jet are listed in Table 1. There is a little difference of the water depth between upstream and downstream of the jet in this case, which can be neglected compared to the results of this paper. The Reynolds number of jet Re_j is defined as:

$$Re_j = \frac{V_j \delta}{\nu} \quad (2)$$

The ratio R of jet to cross flow Reynolds number in Table 1 is defined as

$$R = \frac{Re_j}{Re} \quad (3)$$

Q_c is discharge of the cross flow and Q_j , jet discharge of the nozzle exit.

Numerical Method and Calculation Conditions

The standard version of the two-dimensional κ - ϵ model proposed by Launder and Spalding (1972) is used in this calculation. The flow geometry under consideration and the coordinate system is the same as the experimental case. The calculations using 220×25 nodes in $200\text{cm} \times 10\text{cm}$ zone are performed with finer grids in the region of impingement and near the bottom. The calculation procedure employs a finite volume scheme for the solution of the vertical two-dimensional Reynolds equations.

All the dependent variables are specified at the inflow boundary and the jet exit. The x -component velocity u at the upstream boundary and the y -component v at the jet exit are prescribed from the experimental measurements. The boundary conditions except for the jet exit are prescribed referring to that of Launder and Spalding (1972). At the jet exit, the dependent variables are

Table 1. Experimental Parameters

Q_c (1/s)	U (m/s)	V_j (m/s)	Q_j (1/s)	R
3.96	0.16	0	0	0
		2.88	0.43	0.11
		3.41	0.51	0.13
		4.92	0.74	0.19
		5.70	0.85	0.22

given as follows in this paper:

$$v = V_j, u = 0, k = 0.0001V_j^2 \text{ and } \epsilon = \frac{k^{3/2}}{0.1\delta} \quad (4)$$

The values of the constants in the κ - ϵ model are given with the same complete universality of the constants given by Rodi (1984).

Experimental and Numerical Results

The flow fields of the calculation result with condition of $V_j = 4.97\text{m/s}$ and $U_{in} = 0.16\text{m/s}$ is plotted in Fig. 2. As can be seen, a larger vortex appears at downstream of the jet and a smaller one appears at upstream because of the co-flow produced by the jet and the cross flow. When V_j becoming smaller, the vortex will disappear.

Mean Velocity Distribution

The mean velocity profiles of u for all three series of R in different position are shown in Fig. 3. It can be seen that, for each jet condition, as y increases, the mean velocity decreases continuously from the maximum close to the bottom. A non-dimensional plot is shown in Fig.4 in which the horizontal coordinate is u/u_m and the vertical coordinate is y/b , where b is equal to the value of y at which

$$u = \frac{1}{2}u_m.$$

It is interesting to see that a region is existed where velocity profiles are similar. This results are compared to have a good agreements with the classical profile of the wall jet, referring to the work of Schwartz (1961). Fig. 4 also shows that the similar distribution of the u -velocity ranges all the way from

$$x = 5\text{cm} \text{ (i. e. } \frac{x}{H} = 0.5 \text{)}$$

to

$$x = 20\text{cm} \text{ (i. e. } \frac{x}{H} = 2.0 \text{)}.$$

The similarity of the distribution of u means that in a limited region the flow fields has the same property with plane wall jet. Fig.5 indicates the variations of u_m , the maximum u -velocity in each profile, in terms of V_j , with

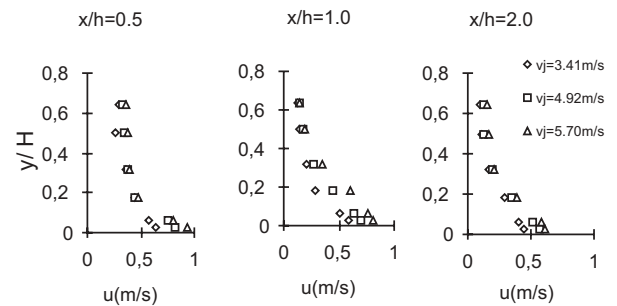


Fig. 3. u -velocity Profile

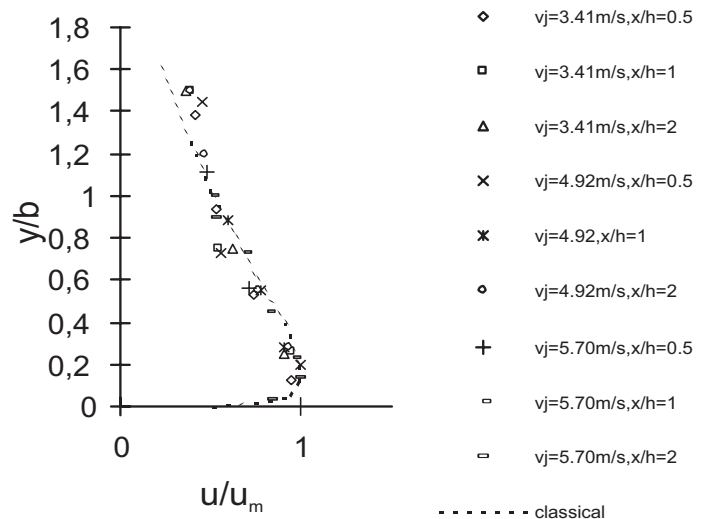


Fig. 4. u -velocity Similarity

$$\frac{x}{H}$$

for $R=0.13, 0.19, 0.22$. For each run of this experiment, the larger of the R , the faster decrease of the u_m with distance of x increase. In addition, the closer the x to the jet impingement point, the faster decrease of u_m . That is to say, high energy dissipation appears near the impingement region.

Turbulent Characteristics

Turbulent intensities of the plane impinging jet in cross flow are measured in the experiments. Some results are plotted in Fig. 6 and Fig. 7 for three series of R . The turbulent intensity distribu-

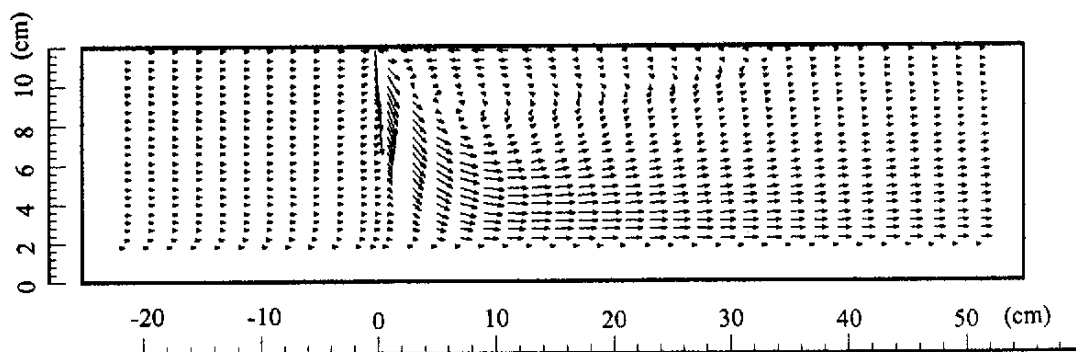


Fig. 2. Flow Field for $V_j=3.41\text{m/s}$, $U=0.16\text{m/s}$

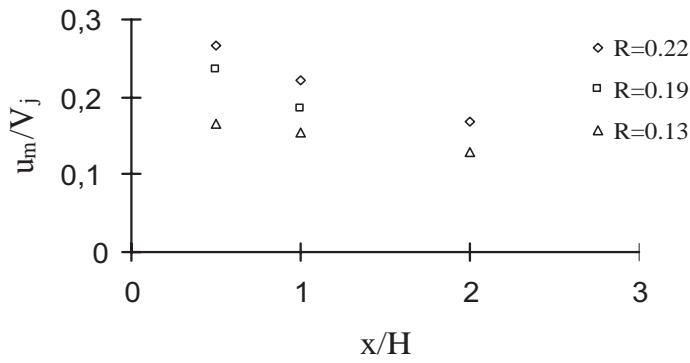


Fig. 5. Variation of the Maximum u-velocity

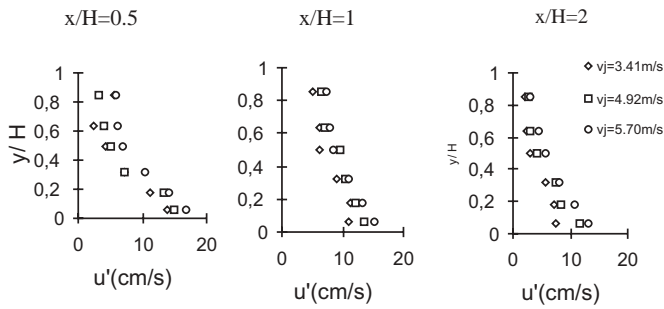


Fig. 6. u' profiles

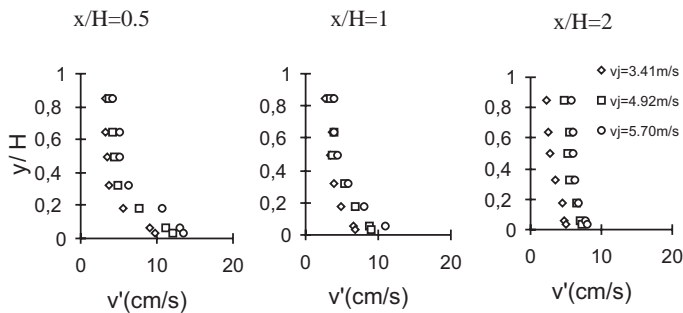


Fig. 7. v' profiles

tions in the region affected by the impingement show different patterns to that of the uniform flow without jet effects. Fig. 8 shows the variations of

$\sqrt{u'^2}$ and $\sqrt{v'^2}$ in a non-dimensional manner at some downstream locations. The turbulent results of the plane wall jet for

$$R = \frac{U_0 b_0}{\nu} = 1.8 \times 10^4$$

measured by Mathieu and Tailland (1965) are plotted herein for comparison, where U_0 and b_0 can be referred to the literature of Mathieu and Tailland (1965). The maximum non-dimensional values of

$\overline{u'^2}$ and $\overline{v'^2}$ in this study are closer to the bottom than that of plane wall jet given by Mathieu and Tailland. For all runs of the experiment, the maximum

$\overline{u'^2}$ and $\overline{v'^2}$ are obtained very near to the bottom where the largest turbulence is produced. Turbulence decays more rapidly as it approaches to the free surface of the cross flow comparing with

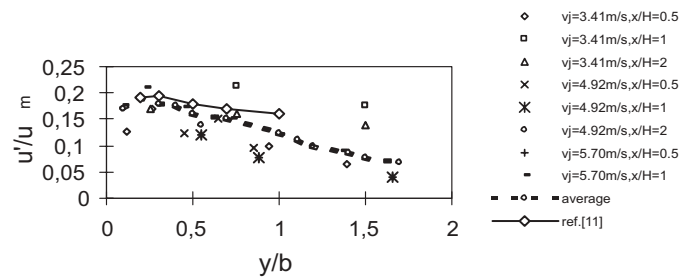


Fig. 8-1. Turbulent Velocity Distribution

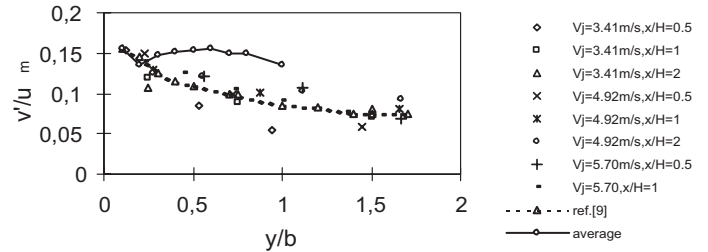


Fig. 8-2. Turbulent Velocity Distribution

the data measured by Mathieu and Tailland, which shows the distinctiveness under this consideration.

In wall-turbulent shear flows, the largest turbulent velocity is approximately 10% of the mean velocity of u (Hinze, 1975). But for the case of this study, violent turbulence appears close to the bottom near the impingement region. The maximum of

$$\frac{\sqrt{u'^2}}{u_m}$$

is approximately equal to 0.20 and that of $\frac{\sqrt{v'^2}}{u_m}$, 0.16. This paper presents the results only in wall jet region of this experiment except for the impingement region because of its complex nature.

Results of the κ - ϵ Model

Corresponding to the experiment conditions, calculations are performed for three forms of the jet velocities with $V_j=3.41\text{m/s}$, 4.97m/s , 5.70m/s and cross flow velocity $U=0.16\text{m/s}$, i. e. Reynolds number ratio $R=0.13$, 0.19 and 0.22 . In this study, it is not the jet to cross flow velocity ratio but the Reynolds number ratio R that has an effect on the flow patterns. The distribution of the time-mean velocity u in the x -direction is shown in Fig. 9 for $R=0.13$. There are also similar u -velocity distributions for the other two R values. The non-dimensional u velocity distribution is shown in Fig. 10 for $R=0.13$, 0.19 and 0.22 . In Fig. 10, some experimental results are also plotted to compare. Fig. 10 obviously shows a similarity of the non-dimensional u velocity distri-

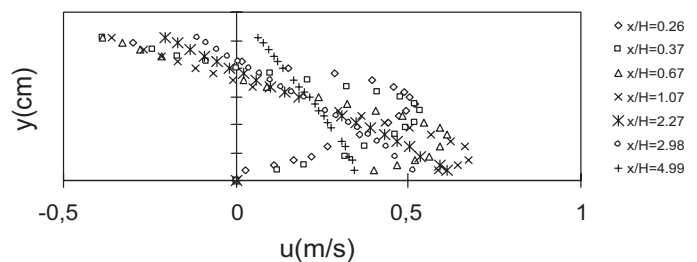


Fig. 9. u -profiles of calculation results ($V_j=3.41\text{m/s}$)

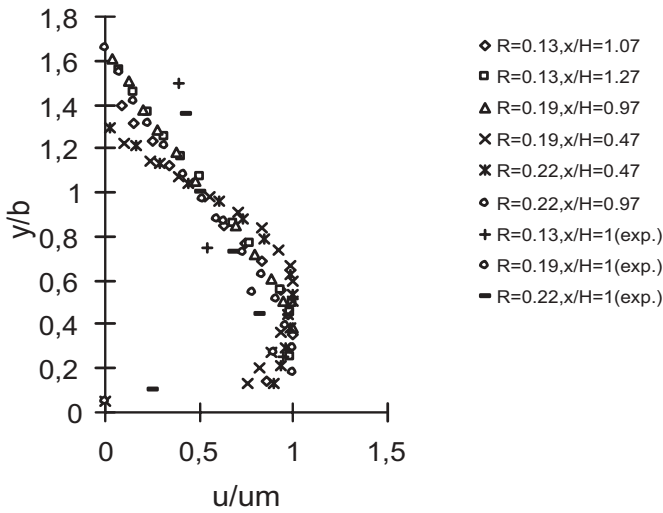


Fig. 10. u -velocity similarity in x -direction

bution as x is close to and great than 5cm (wall jet region), which has a good agreement with the experimental results even though slight scatters exist at upward.

The entire flow of the impingement jet in cross flow may be generally divided into three regions, free jet region, impingement region and wall jet region. Beltaos (1973) has found in his study that the impingement region extends to

$$\frac{x_1}{H} \approx 0.35,$$

and then from that point the wall jet region starts. In this study, it is identified with the similarity property of wall jet that the wall jet region starts from

$$\frac{x}{H} \approx 0.48.$$

It indicates that in the region of

$$\frac{x}{H} < 0.48,$$

the similarity of velocity distribution is not satisfied as can be seen in Fig. 9 and Fig. 10. In Fig. 9 the velocity profiles within $x \leq 3.7\text{cm}$ differ from other curves and also in Fig. 10 even when $x = 4.7\text{cm}$ the non-dimensional curves differ slightly from the others. The impingement point may be located at a farther distance downstream of the jet exit because of the cross flow transport effect on the vertical jet in the streamwise. So the origin of the wall jet region is at lower downstream than that of the impingement jet. Referring to the experimental results of the runs, the origins of the wall jet region start from

$$\frac{x}{H} = 0.5,$$

a slight deviation exists between the results of experiments and computations. In addition, the computational results show that the wall jet region can be kept to

$$\frac{x}{H} = 7.5 \sim 8.9 \quad \text{when } V_j = 5.70 \sim 3.41.$$

Analysis of the results

Maximum u -velocity

Using the method similar to that of the plane turbulent wall jet, the results in the region of the experiment can be described by following equations:

$$u \frac{\partial u}{\partial x} + v \frac{\partial u}{\partial y} = -\frac{1}{\rho} \frac{dp}{dx} + \nu \frac{\partial^2 u}{\partial y^2} + \frac{1}{\rho} \frac{\partial \tau_t}{\partial y} \quad (5)$$

and:

$$\frac{\partial u}{\partial x} + \frac{\partial v}{\partial y} = 0 \quad (6)$$

Using the results of the experimental observations, we could write:

$$\frac{u}{u_m} = f\left(\frac{y}{b}\right) \quad (7)$$

Following a procedure similar to that of Rajaratnam(1976), the equations above can be solved and the correlation is shown as:

$$u_m \propto \frac{1}{\sqrt{x}}, \quad b \propto x \quad (8)$$

Thus we have the rough expressions of the wall jet flow. With a dimensional consideration, an expression of the maximum velocity u_m could be obtained.

Assume that the main parameters under the consideration conditions are momentum of the flux of the cross flow M and that of the jet nozzle M_j , distance x and depth of the flow H , and neglecting the effect of viscosity, we could write:

$$u_m = f_1(M, M_j, x, H) \quad (9)$$

Application of the dimensional analysis and the consideration of u_m decreasing inversely with \sqrt{x} give the following results:

$$\frac{u_m}{U} = f_2\left(\frac{M_j}{M}, \frac{1}{\sqrt{\frac{x}{H}}}\right) = f_2\left(M_r, \frac{1}{\sqrt{\frac{x}{H}}}\right) \quad (10)$$

where M_r is defined as the ratio of M_j and M :

$$M_r = \frac{M_j}{M} = \frac{V_j \delta \cdot V_j}{UH \cdot U} \quad (11)$$

We could rewrite the above equation as:

$$\frac{u_m}{U} = c_1 M_r \frac{1}{\sqrt{\frac{x}{H}}} + c_2 \quad (12)$$

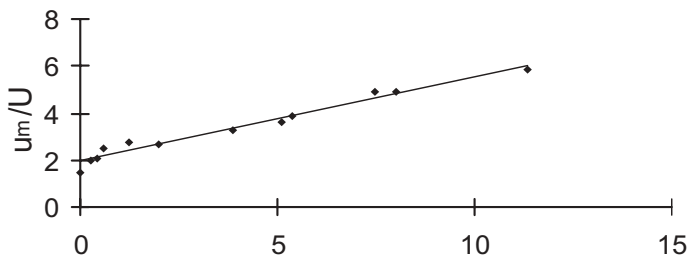


Fig. 11. Variation of u_m

Where c_1 and c_2 are constants which should be decided by experiment. Based on the available experimental data, c_1 is equal to 0.36, and c_2 , 1.96. A similar curve is given as:

$$\frac{u_m}{U} = 0.36 \frac{M_r}{\sqrt{\frac{x}{H}}} + 1.96 \quad (13)$$

This curve, as shown in Fig.11, agrees very well with the experimental data by the least- square fit with a residual value $r_2=0.9909$.

Turbulent Characteristics

The experimental observations for velocity fluctuations u' and v' in a non-dimensional manner of

$$\frac{\sqrt{u'^2}}{u_m}$$

and

$$\frac{\sqrt{v'^2}}{\sqrt{H}}$$

u_m are displayed in Fig. 8 (8-1 and 8-2). The average curve of u' issues somewhat similarity with that of Mathieu and Tailland's, but the average curve of v' is different compared to that of Mathieu and Tailland's. Up to now, turbulence is still difficult to be described by an equation for its complex structure. Nevertheless, more understandings to the turbulence could be increased, which is necessary especially in suspended sediment movement and in practical engineering. In the study cases, the variations of

$$\frac{\sqrt{u'^2}}{u_m}$$

and

$$\frac{\sqrt{v'^2}}{u_m} \frac{y}{b}$$

u_m with b are some similar but different from that of wall jet region (see Rajaratnam,1976). The first difference is that the maximum turbulent velocity for all runs appears at lower positions because of the large ratio R of jet velocity and cross flow velocity. The second is the more rapid decay of the turbulence

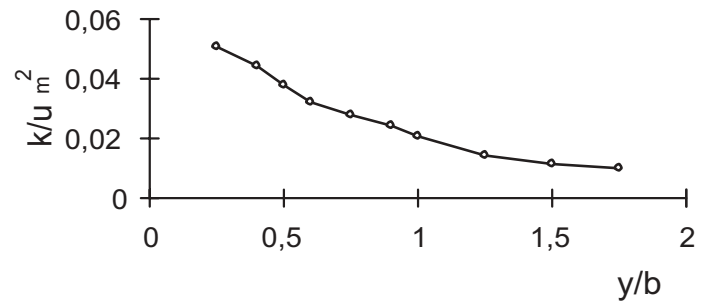


Fig. 12. Turbulent Kinetic Energy Distribution

with the increase of y . Referring to the similarity curve averaged by the experimental data, the turbulent kinetic energy distribution can be obtained as shown in Fig. 12.

Conclusion

The present study has revealed the flow and turbulent structures for a new flow phenomenon of two-dimensional impinging jet downward into a cross flow. This study has its significance as a basis for the further study on the sediment transportation by impinging jet. Summarizing this study leads to the following conclusions:

1. The mean flow starting from a certain position possesses the same property as the wall jet. Similar velocity distributions for series of the ratio R have been shown in this paper.
2. The maximum velocity expression accounting for the momentum ratio of jet and cross flow is obtained by using dimensionless method. The expression formula of the maximum velocity can explain the flow of the two-dimensional vertical impinging jet exactly.
3. The critical point of separating wall jet region and impingement region in the flow of this study is located at the farther downstream of the jet than that of impinging jet in still water reported by Beltaos (1973). The reason is that there is cross flow affection on the jet stream. And the critical point of wall jet region is probably sensitive to the variation of the ratio M_r , which needs further studies. Computation results show that the length of the wall jet region is varied with the ratio of the jet-to-cross flow velocity.
4. The experimental results show that the maximum turbulent fluctuation velocity appears very near the bottom. This velocity structure is a significant effect to prevent solid particles from depositing at the bottom. The impinging jet in cross flow produces more violent turbulence, especially the vertical turbulent velocity,

$$\sqrt{v'^2}$$

Acknowledgment

The authors are thankful to Professor Kazuhiro Fujisaki, Dept. of Civil Eng., Kyushu Institute of Technology, Japan, for reviewing in every detail the earlier and the final draft of this paper. His comments and suggestions are very useful and are included in this paper.

Appendix I. References

- ABRAMOVICH, G.N. (1963), The Theory of Turbulent Jets, English Translation Published by M.I.T. Press, Cambridge, Massachusetts.
- BELTAOS, S. and RAJARATNAM, N.(1977), Impingement of Axisymmetric Developing Jets, Journal of Hydraulic Research, Vol.15, No. 4, pp.311-326.
- BELTAOS, S. and RAJARATNAM, N.(1973), Plane Turbulent Impinging Jets, Journal of Hydraulic Research, Vol.11, No. 1, pp.29-59.
- CHEN ZHICONG, FU RENSHOU, et. al.(1997), The Precautions against Sediment deposition in a Culvert by Impingement Jet, Research Report of Tsinghua University.
- HINZE, J.O.(1975), Turbulence, McGRAW-HILL Company, Second Edition.
- KOBUS, H., LEISTER, P. and WESTRICH, B., Flow Field and Scouring Effects of Steady and Pulsating Jets Impinging on a Movable Bed, Journal of Hydraulic Research, Vol. 17, No. 3, pp. 175-192.
- LAUNDER, B.E. and SPALDING, D.B.(1972), Lectures in Mathematical Models of Turbulence, Academic Press.
- MATHIEU, J. and TAILLAND, A. (1965), Jet Parietal, C. R. Acad. Sci., Paris, 261.
- MCGUIRK, J.J. and RODI, W., A (1978), Depth-averaged Mathematical Model for the Near Field of Side Discharges into Open Channel Flow, J. Fluid Mech., Vol. 86, part 4, pp. 761-781.
- RAJARATNAM, N.(1976), Turbulent Jets, Elsevier Scientific Publishing Company.
- RAJARATNAM, N. and BELTAOS, S.(1977), Erosion by Impinging Circular Turbulent Jets, Journal of the Hydraulics Division, Vol. 103, No. HY10, pp. 1191-1205.
- RODI, W.(1984), Turbulence Models and Their application in

Hydraulics - a State of the Art Review, Intsitut für Hydro-mechanik University of Karlsruhe, Germany.

- SCHWARTZ, W.H. and COSART, W.P.(1961), The Two-Dimensional Turbulent Wall Jet, J. Fluid Mech., Vol. 10, pp. 481-495.

Appendix II. Notation

The following symbols are used in this paper:

b	half width where $u = \frac{u_m}{2}$;
c_1 and c_2	constants;
H	the depth of the flume flow;
M	flux momentum of the cross flow;
M_j	flux momentum of the jet nozzle;
M_r	the ratio of M_j to M ;
p	pressure;
Q_c	cross flow discharge;
Q_j	jet nozzle discharge;
R	Reynolds number ratio of jet to cross flow;
R_e	Reynolds number of the cross flow;
R_{ej}	Reynolds number at jet nozzle;
U	mean inlet velocity of the cross inlet flow;
u	time-averaged streamwise velocity;
u_m	maximum velocity of u at cross section;
$\sqrt{u'^2}$ and $\sqrt{v'^2}$	turbulent intensities;
v	time-averaged vertical velocity;
x, y	coordinate axes;
ν	fluid kinematic viscosity;
δ	jet nozzle width;
ρ	fluid density; and
τ_t	shear stress;